Published in final edited form as:
Clin Cancer Res. 2011 March 15; 17(6): 1405–1414. doi:10.1158/1078-0432.CCR-10-1614.

Effect of Zoledronate on Oral Wound Healing in Rats

Junro Yamashita[1], **Kiyono Koi**[1], **Dong-Ye Yang**[1], and **Laurie K. McCauley**[2,3]

[1]Department of Biologic Materials and Sciences, School of Dentistry University of Michigan, Ann Arbor, Michigan

[2]Department of Periodontics and Oral Medicine, School of Dentistry, University of Michigan, Ann Arbor, Michigan

[3]Department of Pathology, Medical School University of Michigan, Ann Arbor, Michigan

Abstract

Purpose—Osteonecrosis of the jaw (ONJ) is a growing concern in patients who receive bisphosphonates which target osteoclasts. Since osteoclasts play multifunctional roles in the bone marrow, their suppression likely affects bone homeostasis and alters wound healing of the jaw. The objective was to delineate the impact of osteoclast suppression in the bone marrow and wound healing of the jaw.

Experimental Design—Zoledronate was administered to senile rats for 14 weeks. A portion of the gingiva was removed to denude the palatal bone. Gene expression in the bone marrow was assessed and histologic sections analyzed to determine the wound healing status.

Results—Angiogenesis-related genes, CD31 and VEGF-A, were not altered by zoledronate. VEGF-C, which plays a role in lymphangiogenesis, was suppressed. There was a decrease in gene expression of Tcirg1 and MMP-13. Bone denudation caused extensive osteocyte death indicative of bone necrosis. In zoledronate-treated rats, the necrotic bone was retained in the wound while, in controls, osteoclastic resorption of the necrotic bone was prominent. Even though large necrotic bone areas existed in zoledronate-treated rats, overlaying soft tissue healed clinically. Immunohistochemical staining showed rich vascularity in the overlaying soft tissue.

Conclusions—Zoledronate therapy impacts bone marrow by suppressing genes associated with lymphoangiogenesis and tissue remodeling, such as VEGF-C and MMP-13. Zoledronate was associated with impaired osseous wound healing but had no effect on angiogenic markers in the bone marrow or soft tissue wound healing. Zoledronate selectively blunts healing in bone but does not effect soft tissue healing in the oral cavity.

Introduction

Nitrogen-containing bisphosphonates (N-BPs) are administered intravenously to patients for the treatment of metastatic cancer, hypercalcemia of malignancy, Paget's disease and osteoporosis (1). N-BPs potently suppress osteoclastic bone resorption, thereby reducing the occurrence of skeletal-related events, such as pathologic bone fractures and associated pain in patients with malignant bone diseases (2). A recent report further suggests that N-BPs

Corresponding author: Junro Yamashita 1011 N. Univ. Ave., Ann Arbor, MI 48109-1078, University of Michigan School of Dentistry Tel: 734-764-0238; Fax: 734-647-2110 yamashit@umich.edu.
yamashit@umich.edu
koi@umich.edu
yangdy@umich.edu
mccauley@umich.edu

have anti-tumor effects independent of osteoclastic bone resorption as the administration of zoledronate, the most potent N-BP, suppressed tumor growth in bone where osteoclasts were functionally defective (3). Although the clinical benefit of N-BPs in the treatment of cancer metastasis is well-recognized, recent reports indicate that chronic N-BP therapy, especially zoledronic acid, is associated with the development of osteonecrosis of the jaw (ONJ) (4,5).

Osteoclasts are of hematopoietic origin and play a pivotal role in the maintenance of the hematopoietic system in bone (6). Osteoclast precursors share biological functions with immune cells, such as macrophages and dendritic cells (7,8). Similar to macrophages, osteoclasts and their precursors secrete cytokines in response to proinflammatory signals which chemoattracts other immune cells to inflammatory sites (9-11). Thus, osteoclasts and precursors participate in the resolution of inflammation in and around bone. Osteoclasts are also involved in angiogenesis, expressing angiogenic factors such as VEGF, angiopoietin-1, -2, and MMP-9 at modeling and remodeling sites (12-14). Osteoclastic bone resorption is followed by angiogenesis in the bone matrix. Osteoclast suppression decreases angiogenesis in bone while enhanced osteoclastogenesis increases angiogenesis (15). Considering the multifunctional role of osteoclasts, chronically suppressed osteoclasts by N-BPs would have extensive influence over the cellular environment in bone. However, effects of long-term osteoclast inhibition in the bone environment have not been fully examined. While such an altered cellular environment in bone could hamper tumor metastasis, it may have an adverse effect on bone homeostasis. ONJ, which is a rare but serious adverse event associated with N-BP therapy, may be attributed to the altered cellular environment in bone caused by osteoclast inhibition. In this study, we hypothesized that long-term cancer-dose zoledronate therapy influences the cellular environment in bone and alters wound healing properties of the craniofacial bone. Zoledronate was administered to senile rats at the same time an oral trauma was created. Gene expression in the bone marrow and healing of oral wound were assessed. Zoledronate significantly suppressed genes associated with macrophages and lymphangiogenesis in the bone marrow and impaired alveolar bone wound healing. The result of this study demonstrates that long-term zoledronate therapy alters cellular environments in bone and has a negative impact on osseous healing of the jaw.

Materials and Methods

Animals, injections, and palatal bone denudation

The experimental design and protocol were reviewed and approved by the University Committee on Use and Care of Animals. Twenty-four (senile: one year old female) and sixteen (young: 5 week old male) Sprague Dawley rats were obtained from a commercial vendor (Charles River Laboratories, Wilmington, MA). Rats were fed with standard rodent diet. The potent N-BP, zoledronate (Zometa, Novartis, Basel, Switzerland) was used. A subcutaneous dose of 0.3mg/kg/week of zoledronate divided into two doses was used in the high-dose group (HZA) and 0.1mg/kg/week divided into two doses in the normal-dose group (ZA). These doses were selected since the dose for rodent proof-of-concept studies is approximately 0.1mg/kg/week (16,17). The high-dose of 0.3mg/kg/week was used to study adverse effects of zoledronate. An equivalent volume of saline was injected for the vehicle control group (VC). At 12 weeks after the initiation of zoledronate therapy, palatal wounds were created to assess the effect of zoledronate on healing of the denuded palatal bone (Fig. 1A). Senile rats were anesthetized and the palatal mucosa between the first molar (M1) and the great palatine canal (GPC) was excised using a curette to denude the alveolar process of the palatal bone (Fig. 1B). The size of the excised palatal mucosa was approximately 3 × 1.5 mm. The denuded palatal bone was left exposed to study spontaneous wound healing. Each group consisted of 8 senile rats and subcutaneous injections were carried out twice a week for 14 weeks. All senile rats were euthanized at week-14. Young rats were subjected to either subcutaneous injections of 0.3mg/kg/week of zoledronate divided into five doses or an

equivalent volume of saline for 10 days. Young rats were euthanized one day after the last injection.

Serum chemistry

Blood (0.05 mL) was collected from the tail vein of senile rats every 4 weeks to obtain serum. Serum was kept at −80°C until use. Serum TRAcP5b, calcium, intact parathyroid hormone (iPTH), procollagen type I N-terminal propeptide (P1NP) were measured to assess bone resorption and formation activity using commercially available kits (RatTRAP Assay, IDS, Boldon, UK; Calcium assay, Pointe Scientific, Canton, MI; iPTH assay, Alpco, Salem, NH; Rat/Mouse P1NP, IDS).

Long bone mineral density and histomorphometry

Right femurs and tibiae of senile rats were fixed in 10% formalin and kept in 70% ethanol. Peripheral Quantitative Computed Tomography (pQCT) scanning to measure bone mineral density (BMD) in the metaphysis and diaphysis of the distal femur was performed using XCT Research SA+ (Stratec, Pforzheim, DE). A transverse pQCT slice was taken at the distal 20% position of the total femur length. Tibiae were decalcified in 10% ethylenediaminetetraacetic acid (EDTA), embedded in paraffin, sectioned, and stained for Masson's Trichrome and tartrate-resistant acid phosphatase (TRAP) using commercial kits (HT15 and 386A, Sigma-Aldrich, St. Louis, MO). The stained sections were histomorphometrically analyzed using Image-Pro Plus v4 (Media Cybernetics, Silver Spring, MD). Bone tissue within 10mm from the growth plate of the proximal tibiae was assessed for bone area (%) and empty osteocyte lacunae. Numbers of empty and non-empty osteocyte lacunae within the cortex were counted and their ratio determined. Osteoclast number and trabecular bone perimeter were calculated in the proximal tibia to determine osteoclast numbers (#/mm) as described before (18).

Quantitative real-time PCR

Senile rats were euthanized at 14 weeks and the bone marrow isolated from the humeri directly into TRIZOL (Invitrogen, Grand Island, NY) using centrifugation (19). Total RNA was extracted by the phenol/chloroform method. First-strand cDNA was synthesized using the SuperScript First-strand system (Invitrogen). Quantitative real-time PCR (qRT-PCR) was performed using an iCycler IQ (BioRad, Hercules, CA) with SYBRGreen mix (Invitrogen). Samples were run in triplicate and results normalized to 18S expression. The sets of primers used for real-time PCR were: 18S, 5′-GTTGGTTTTCGGAACTGAGGC-3′ and 5′-GTCGGCATCGTTTATGGTCG-3′; T-cell immune regulator 1 (Tcirg1), 5′-GCCTTTGCTGTGTTGACTGT-3′ and 5′-GTTCTGGAACTCCACCCAGT-3′; platelet/endothelial cell adhesion molecule-1 (CD31), 5′-CCGCCTTGATAGTTGCAGCCAAAT -3′ and 5′-AATGGCTGTTGGTTTCCACACTGG -3′; Vascular endothelial growth factor-a (VEGF-A), 5′-TTGAGACCCTGGTGGACATC-3′ and 5′-CTACCAAAGTTCCCCCTCTC-3′; monocyte/macrophage antigen CD68, 5′-TTCTCCAGCAATTCACCTGGACCT-3′ and 5′-AGGCAGCAAGAGAGATTGGTCACT-3′; EGF-like module containing, mucin-like, hormone receptor-like sequence 1 (EMR1), 5′-CCTTCAAGGCCATTGCCCAGATTT-3′ and 5′-ATGCCATTATGCTTGCCAAGGGAC-3′; Matrix Metalloproteinase 13 (MMP-13), 5′-ACTTGTGTGACAGGAGCTAAGGCA-3′ and 5′-AGGAGCATGAAAGGGTGGTCTCAA-3′; Vascular endothelial growth factor-c (VEGF-C), 5′-GCAACATTACCACACGTGTCAGGCA-3′ and 5′-ACTCCTTGTTGGGTCCACAGACAT-3′; CXCR4, 5′-CTCCAAGCTGTCACACTCCA-3′ and 5′-TCCCCACGTAATACGGTAGC-3′; CXCL12, 5′-GCTCTGCATCAGTGACGGTA-3′ and 5′-CAGCCTTGCAACAATCTGAA-3′.

The bone marrow was isolated from the jaw and femur of young rats at day-11 and total RNA extracted using the same protocol written above. qRT-PCR was performed to analyze the gene expression for Tcirg1, VEGF-C, and MMP-13.

Palatal wounds and immunohistochemistry

At the study end (2 weeks after oral bone denudation), the palates were removed and fixed in 10% formalin. The palatal bones were decalcified in 10% EDTA, embedded in paraffin, sectioned, stained for Masson's Trichrome and TRAP, and histomorphometrically analyzed. The area of interest (AOI) was defined as the bone area within 1.0 mm from the palatal bone surface between the M1 and GPC (Fig. 1C). Numbers of empty and non-empty osteocyte lacunae were counted in each AOI in trichrome-stained sections and their ratio determined. Osteocyte analyses were completed for the contralateral AOI where no surgery was performed. Osteoclast perimeter (#/mm) was determined in each AOI in TRAP-stained sections. In this study a portion of bone in which greater than or equal to 10 adjacent empty osteocyte lacunae was defined as necrotic bone since such bone is devital (20). Therefore, small areas with less than 10 neighboring empty osteocyte lacunae were not counted as necrotic bone. The size of necrotic bone area was histomorphometrically measured using Image-Pro Plus v4 and compared between HZA and VC. The expression of von Willebrand factor (vWF) and CD68 in the connective tissue next to the AOI were immunohistochemically analyzed to assess blood vessels and macrophages in wounds, respectively. Sections were deparaffinized and enzymatic epitope retrieval was performed in 0.05% trypsin. Nonspecific protein was blocked with 10% goat serum. Sections were incubated at 4°C overnight with a mouse monoclonal CD68 antibody (MAB1435, Millipore, Billerica, MA) and a rabbit polyclonal vWF antibody (ab6999, Abcam, Cambridge, MA). Endogenous peroxidase activity was blocked with 0.3% hydrogen peroxide. Goat anti-mouse IgG (AP340P, Millipore) and anti-rabbit IgG (AP307, Millipore) conjugated to horseradish peroxidase were used for secondary antibodies and proteins developed with DAB (Vector Laboratories, Burlingame, CA). Sections were counterstained with hematoxylin and mounted. Numbers of vWF+ blood vessels and CD68+ cells per mm^2 in the oral mucosa next to the AOI were histomorphometrically assessed and compared.

Statistical analysis

Data were analyzed for equality of variances. Independent samples t-tests for two groups, paired samples t-test, and one-way ANOVA for multiple groups were performed for parametric data. Tukey's test was used for a post-hoc analysis. For non-parametric paired data, Wilcoxon rank sum test was used. All statistical analysis was calculated with SPSS v16 (SPSS, Chicago, IL) using an alpha level of 0.05. Results are presented as mean ± SE (standard error) unless specified.

Results

Zoledronate suppressed osteoclasts without altering the gross bone structure

Body weight was monitored to detect possible systemic side effects of high dose zoledronate administration. Two-way repeated-measures ANOVA revealed no significant difference between groups in weight change (data not shown). pQCT bone assessment was performed to examine the effect of zoledronate on bone at the tissue level and revealed no differences in BMD at the metaphysis and diaphysis of the femurs between HZA, ZA, and VC rats (Fig. 2A). Consistently, histomorphometric analysis of the proximal tibiae showed that bone area (%) was similar in all groups (Fig. 2B). The ratio of the number of empty osteocyte lacunae to total osteocyte lacunae was assessed in the cortex of the proximal tibiae and there were no significant differences between zoledronate-treated and VC rats (Fig. 2C). For insight into bone formation/resorption in zoledronate-administered senile rats, serum chemistry was

assessed. Average serum TRAcP5b levels dropped significantly in both HZA and ZA rats compared to VC rats (Fig. 2D). As anticipated from the TRAcP5b result, HZA and ZA rats showed significantly lower osteoclast perimeters compared to VC rats (Fig. 2E). Assessment of serum Ca levels at day-0 and week-12 showed significantly reduced Ca level in HZA but not in ZA rats (Fig. 2F). No difference was noted in the serum Ca levels between ZA and VC rats. Since reduced calcium levels due to osteoclast suppression in ZA rats could be compensated by other endocrine mechanisms, we analyzed intact PTH (iPTH) levels in the serum; however, no statistical differences were found between groups (Fig. 2G). Thus, the high-dose zoledronate administration, but not the normal dose, had a sustained effect on calcium. Serum P1NP levels, a marker of bone formation (21), were also assessed since osteoclast inhibition could suppress osteoblast activity via coupling (22). It was revealed that the P1NP levels were significantly lower in ZA rats compared to those in VC rats (Fig. 2H). However, no reduction was noted in HZA rats.

Zoledronate suppressed Tcirg1, VEGF-C, and MMP-13 in the bone marrow

To investigate the effect of long-term zoledronate therapy on the bone marrow micro-environment, total RNA was isolated and genes associated with macrophages, angiogenesis, and cancer metastasis were assessed using qRT-PCR (Fig. 3A). As the bone marrow isolation from the jaw was technically difficult to perform due to the densely calcified cortex and small marrow size in senile rats, the bone marrow from the humeri was analyzed instead. To verify whether 18S expression was altered by zoledronate therapy, gene expression was normalized to GAPDH expression and results compared. No differences were noted in the normalized gene expression between 18S and GAPDH (data not shown). The expression of Tcirg1, a gene critical for immune activation and osteoclast function (23,24), was significantly suppressed in HZA and ZA rats. CD68 and EMR1, markers of cells in the macrophage/monocyte lineage (25), were also found altered. The expression of CD68 was significantly suppressed in HZA rats and while no statistical difference was noted in the expression of EMR1, there was a trend that it was decreased with ZA treatment. Since angiogenesis is a critical component of bone remodeling and cancer metastasis, angiogenic-related genes, CD31, VEGF-A, and VEGF-C were examined. No alterations were noted in the expression of CD31 or VEGF-A by zoledronate treatment. However, VEGF-C which is strongly associated with lymphangiogenesis was significantly suppressed in both HZA and ZA rats. Because zoledronate is approved to treat cancer bone metastasis and is effective in the suppression of skeletal-related events, we assessed MMP-13, CXCL12, and CXCR4, genes involved in cancer metastasis to bone (26,27). Zoledronate therapy significantly suppressed MMP-13, which plays a role in tumor-induced osteolysis, in both HZA and ZA rats. The expression of CXCL12 and CXCR4 were significantly reduced in HZA but not in ZA rats.

To get an insight into a similarity or a difference between the humerus and jaw in the bone marrow cellular responses to zoledronate, young rats were subjected to zoledronate administration for 10 days and gene expression assessed for Tcirg1, MMP-13, and VEGF-C. Young rats were chosen because they have a large bone marrow space in the alveolar bone of the jaw to isolate for molecular analysis. Although young rats and short-term zoledronate therapy were used, it was found that MMP-13 and VEGF-C were significantly suppressed by zoledronate therapy in the bone marrow of both the femur and jaw (Fig. 3B). As for Tcirg1, the expression was significantly suppressed in the jaw but there was no notable difference in the femur.

Wound healing in the palate

Wound healing in the palate was assessed to investigate the effect of zoledronate on healing of the jaw bone and mucosa. It was also aimed to examine an association between the

altered bone marrow environment and bone wound healing in the maxilla. Since atraumatic molar tooth extraction is difficult to perform in 1-year-old rats due to excessive cementum apposition on the roots (28,29), an oral trauma model was employed instead. The palatal bone was denuded after 12-weeks of VC, ZA or HZA treatment and healing assessed 2 weeks later. Gross observation of wound healing revealed no difference between HZA, ZA, and VC rats; epithelialization was generally observed and no exposed bone noted. To scrutinize wound healing, trichrome-stained sections were histomorphometrically assessed. With trichrome staining, collagen, fibrin, erythrocytes, and muscle are distinctively identified and nucleus distinguished (30). In all groups, wound sites exhibited a thin stratum corneum, narrow width of stratum spinosum without rete pegs, and loose collagenous connective tissue (Fig. 4A, B). The shape of the palatal bone in the wound was quite different between zoledronate-treated and VC rats. Zoledronate-treated rats maintained the original shape of the palatal bone in the denuded area, while the margin of the palatal bone was irregular in VC rats due to bone resorption. In HZA and ZA rats, intense neutrophil aggregation was observed in the connective tissue directly next to the once denuded bone surface. However, in VC rats, neutrophil aggregation was noted only near bone surfaces where no bone resorption took place and no neutrophil aggregation was seen next to the bone surfaces where bone resorption had already occurred. Thus, intense inflammation was ongoing in HZA and ZA rats but not VC rats. Observation of the palatal bone with higher magnification revealed that most of osteocyte lacunae in the denuded side were either empty or contained shrunken osteocytes while osteocytes appeared normal in the contralateral side where no trauma was induced regardless of the group. Histomorphometric analysis of osteocyte lacunae in the pre-defined AOI showed that approximately 70% of osteocyte lacunae were empty in the denuded side and less than 20% in the contralateral side regardless of treatment (Fig. 5A). Therefore, the palatal alveolar bone in the AOI of the denuded side was mostly devital, hence necrotic, in both zoledronate- and vehicle-treated rats. To determine the influence of zoledronate therapy on the susceptibility to bone necrosis triggered by bone denudation, the extent of necrotic bone, not only within the AOI but also in the entire alveolar bone, was assessed in HZA rats. It was found that necrotic bone area was significantly larger in HZA than control (Fig. 5B). Thus, bone necrosis occurred considerably more in zoledronate-treated rats than in VC rats when the jaw bone was denuded. To assess the role of osteoclasts in wound healing, osteoclast perimeter was determined in the AOI of TRAP-stained sections. Osteoclast perimeter was significantly reduced in zoledronate-treated versus VC rats (Fig. 5C). In VC rats, osteoclasts were observed exclusively on the irregular bone surface (Fig. 4C left). This suggests that the necrotic palatal bone was not being removed by osteoclasts in zoledronate-treated rats while the necrotic bone was being removed in VC rats. Furthermore, neutrophil aggregation was attenuated near the bone surfaces where osteoclasts were detected. Hence, although the denuded jaw bone was covered by oral mucosa and therefore wound healing appeared normal clinically, underneath the necrotic palatal alveolar bone an inflammatory cell aggregation persisted in zoledronate-treated rats. To obtain insight into reduced osteoclast perimeters in zoledronate-treated rats, preosteoclasts (TRAP+ mononuclear cells) in the connective tissue of the wounds were quantified. Preosteoclast numbers per mm^2 were significantly reduced in zoledronate-treated rats versus VC rats, indicating that zoledronate treatment suppressed not only mature osteoclasts but also osteoclast precursors (Fig. 5D). Preosteoclasts were hardly detectable in the contralateral intact sides in all groups.

To further characterize impaired mucosa healing in zoledronate-treated rats, blood vessels and macrophages were assessed. There were no differences in vWF-stained blood vessel numbers between HZA, ZA, and VC rats in the denuded or contralateral intact side (Fig. 5E). When the vessel number was compared between the denuded and contralateral intact side, the denuded side exhibited more blood vessels than the contralateral intact side in all groups ($p < 0.01$ for ZA and $p < 0.05$ for HZA and VC). The connective tissues in wounds

were rich in blood vessels in all groups (Fig. 4C middle). Thus, no obvious effects of zoledronate treatment on blood vessels were noted in the connective tissue of the palates. While, no statistical differences were detected in CD68+ cells between groups in the denuded or contralateral intact side (Fig. 5F), significantly more CD68+ cells were noted in the denuded side than in the contralateral intact side, suggesting comparable inflammatory response in the wound area in all groups.

Discussion

Zoledronate has a strong affinity to bone mineral and exerts anti-resorptive effects by targeting osteoclasts (31). Since osteoclasts play an important role in hematopoiesis, chronically suppressed osteoclasts would likely alter cellular responses during wound healing (6). This could be in connection with the development of the ONJ. In this study cancer-dose zoledronate was administered to senile rats and oral lesions created to comprehend underlying mechanisms behind the development of ONJ.

Zoledronate administration had no obvious effect on structural bone parameters in hindlimbs, as shown in the BMD and bone area analyses, however, osteoclasts were significantly suppressed as evidenced by a reduction in serum TRAcP5b levels and osteoclast numbers. The lack of alteration in the structural bone parameters is likely due to slow bone turnover in senile rats. In a preliminary experiment, zoledronate prevented bone loss from ovariectomized senile rats (data not shown), thus, zoledronate administration suppressed osteoclasts throughout the treatment period and such continuously suppressed osteoclasts were found to have an impact in the bone marrow. In this study the marrow of the long bone was assessed as a surrogate for the bone marrow of the jaw in senile rats. This was because the bone marrow isolation from the jaw is not feasible due to the dense cortex and a substantially small bone marrow space in senile rats. To validate whether their cellular responses to zoledronate are similar, gene expression was compared between the long bone and jaw using young rats. Previous studies using rodents indicates that zoledronate exerts its effect on bone wound healing (32) or osteolytic bone metastases (33) as early as 10 days when administered daily. Although in such studies relatively high doses of zoledronate (approximately 1.0~1.75 mg/kg/week) were used, in this study 0.3mg/kg/week of zoledronate divided into five doses was enough to alter gene expression in the bone marrow. We found that the expression of MMP-13 and VEGF-C was comparable between the long bone and jaw in response to zoledronate. In contrast, Tcirg1 was suppressed in the jaw but not suppressed in the long bone. Although precise reasons for this are unknown, zoledronate therapy for 10 days may not be long enough to suppress Tcirg1 expression, alternatively the low basal levels of Tcirg1 in young rats may render further suppression unlikely. It is possible that differences in the animal age and administration regimen between senile and young rats could have affected the overall gene expression profile in the bone marrow.

In the current study the expression of immunomodulatory genes including Tcirg1 and CD68 were suppressed. MMP-13 which is important in tissue remodeling was also suppressed. Previous studies have shown that zoledronate has anti-angiogenic properties, thereby interfering with tumor growth *in vivo* (34). However, this is still open to discussion. Santini et al. reported reduced serum VEGF levels following zoledronate administration (35). In contrast, Tas et al. showed no decrease in serum VEGF levels (36). In the current study, no alteration was found in the expression of CD31 and VEGF-A in the bone marrow. This suggests that zoledronate may not impact angiogenesis in the native bone marrow. The expression of VEGF-C was significantly suppressed. VEGF-C plays a role in the formation of lymphatic vessels (37) which drain tissue fluid, thereby reducing edema during wound healing or inflammation. A link between bisphosphonates and the impaired lymphatic system in the bone was recently reported. Li et al. investigated the effect of antiresorptive

agents on the pathogenesis of bone infection and reported that alendronate caused a reduction in draining lymph node volume with exacerbated osteomyelitis (38). Their finding is in parallel with our finding that long-term zoledronate therapy suppressed VEGF-C but not CD31 and VEGF-A in the bone marrow, and suggests that impaired wound healing with bisphosphonates may be associated with compromised lymphoangiogenesis.

The denudation of the palatal bone induced an intensive local inflammatory response and resulted in death of osteocytes in the involved bone region. Osteocyte death likely resulted from local ischemia due to loss of the periosteum and connective tissue. Such trauma-induced localized bone necrosis occurred in both zoledronate-treated rats and controls. When a portion of the bone gets necrotic, it is typically removed and replaced with new bone. This repair process depends on osteoclasts. In this study, bone resorption took place in vehicle control rats only. Minimal bone resorption of necrotic bone, if any, occurred in zoledronate-treated rats. Neutrophils arrive at an injured tissue site first to sterilize the lesion then send signals to macrophages to orchestrate repair (39). As macrophages and other immune cells arrive, neutrophil aggregation subsides. In the palatal wounds, disappearance of neutrophil aggregation was observed only in control, with sustained aggregation in zoledronate-treated rats since necrotic bone was retained due to osteoclast inhibition. Interestingly, the frequency of empty osteocyte lacunae in the intact palatal bone was much higher than that in the cortex of the proximal tibiae (approximately 18% in the palate versus 2% in the proximal tibia). This suggests that the jaw requires more frequent remodeling than the long bone in physiological conditions. The jaw is subjected to many mechanical stresses during mastication. Such stresses induce microdamage leading to osteocyte death, which necessitates local bone remodeling (40). In fact, the bone remodeling rate is thought to be high in the jaw throughout life compared to the femur (41). Therefore, the suppression of bone turnover by zolendronate may have more profound effects on the jaw than in the long bones. This study also found no difference in the frequency of empty osteocyte lacunae in the contralateral side of the palates between control and zoledronate-treated groups. On the other hand, on the denuded side, necrotic bone area was significantly more extensive in zoledronate-treated rats than control. This implies that zolendronate may have the potential to exacerbate bone damage. When bone becomes necrotic, bone repair is initiated by osteoclasts. However, due to osteoclast suppression by zoledronate, necrotic bone persists in the region. Such a continued existence of necrotic bone may have a negative effect on surrounding bone leading to the expansion of bone necrosis. An alternative explanation for this is that long-term zoledronate therapy suppresses osteocyte viability (42). Although cytotoxic effects of zoledronate have been reported (43), its effect on osteocytes remains unknown. Since our study found no differences in the frequency of empty osteocyte lacunae in the contralateral side as well as in the proximal tibiae, it is unlikely that zoledronate therapy exerted a cytotoxic effect on osteocytes in the rats in this study.

In the marrow of the long bone, the expression of CD68 was suppressed in zoledronate-treated rats. However, in oral wounds CD68+ cells (macrophages) were not suppressed by zoledronate therapy and macrophages were attracted to the inflammation site similar to control. Since CD68 is expressed in osteoclasts as well (44), suppressed CD68 expression in the bone marrow might be a reflection mainly of suppressed osteoclasts. This may explain the discrepancy in findings between CD68 in the bone marrow and in the oral wounds. In the palatal lesions of control rats some CD68+ cells seemingly differentiated into osteoclasts, but in zoledronate-treated rats, minimal osteoclast differentiation took place. Pre-osteoclasts (TRAP+ mononuclear cells) were also scarce in zoledronate-treated rats, while in control many pre-osteoclasts were observed near the resorbing surface of bone. No giant osteoclasts, as has been described in humans, were noted in zoledronate-treated rats (45). It is not clear in this study whether osteoclast differentiation was perturbed or osteoclasts were discharged after their contact with zoledronate-attached mineral surfaces.

Nonetheless, our histological observation suggests that osteoclast differentiation might be impaired from the early differentiation stage of myeloid cells into pre-osteoclasts in oral wounds. Surprisingly, gross healing of oral mucosa, on the other hand, appeared to be normal in both zoledronate-treated rats and controls. Even though a dense neutrophil layer existed in connective tissue over the necrotic bone, oral wounds were covered by epithelium in both zoledronate-treated and control rats. One explanation for this soft tissue healing is vascularity in zoledronate-treated rats. Angiogenesis is essential in wound repair and suppressed angiogenesis results in impaired wound healing (46). We visualized vWF+ endothelial cells in histological sections and found rich vascularity with no difference in blood vessel numbers between zoledronate-treated and control rats. Therefore, zoledronate appears to have no obvious anti-angiogenic effect in rat oral wounds. This is significant because bisphosphonates are often considered to suppress angiogenesis and to have soft tissue toxicity (34,47). Since our study assessed wound healing at 2 weeks in rats, it is not clear what would transpire relative to repair of the palatal necrotic bone over time. Considering that zoledronate adheres to bone with a half life of many years, osteoclastic resorption of the necrotic bone is unlikely to happen immediately. This could result in the retention of chronic inflammation in connective tissue. It is possible that the retained necrotic palatal bone would be exposed easily if the overlying soft tissue was thin, easily traumatized and/or infected.

In summary, this study showed evidence that long-term cancer-dose zoledronate administration has an impact in the bone marrow cellular environment and wound healing of oral lesions. In our model, zoledronate induced impaired osseous wound healing of the jaw and the retention of inflammation in connective tissue but gross soft tissue healing appeared normal. Lastly, our results suggest that zoledronate has no effect on blood vessel formation in oral wounds.

Statement of Translational Relevance

The multifunctional roles of osteoclasts have recently been emphasized. In addition to bone resorption, osteoclasts are involved in hematopoietic progenitor cell trafficking, immune responses, and angiogenesis. Zoledronate, which is widely used for the treatment of metastatic bone disease, potently inhibits osteoclasts. Hence, long-term osteoclast suppression by zoledronate therapy is likely linked to the development of osteonecrosis of the jaw (ONJ) where osseous wound repair is severely impaired. This work reports that zoledronate may alter the bone marrow cellular environment by targeting genes associated with lymphangiogenesis and bone remodeling. Although such a change would be beneficial for cancer therapy, our work discovered that zoledronate therapy impedes osseous wounds repair of the jaw without altering soft tissue wound healing. These results suggest it would be valuable to establish optimal zoledronate administration protocols that minimize its negative impact on osseous wound healing.

Acknowledgments

Grant Support:

This study was supported by the International Team for Implantology (ITI) grant SGA510, NCI P01-CA093900, and NIDCR grant R03DE018923

References

1. Black DM, Delmas PD, Eastell R, et al. Once-yearly zoledronic acid for treatment of postmenopausal osteoporosis. N Engl J Med. 2007; 356:1809–22. [PubMed: 17476007]

2. Costa L, Major PP. Effect of bisphosphonates on pain and quality of life in patients with bone metastases. Nat Clin Pract Oncol. 2009; 6:163–74. [PubMed: 19190592]

3. Hirbe AC, Roelofs AJ, Floyd DH, et al. The bisphosphonate zoledronic acid decreases tumor growth in bone in mice with defective osteoclasts. Bone. 2009; 44:908–16. [PubMed: 19442620]

4. Marx RE. Pamidronate (Aredia) and zoledronate (Zometa) induced avascular necrosis of the jaws: a growing epidemic. J Oral Maxillofac Surg. 2003; 61:1115–7. [PubMed: 12966493]

5. Ruggiero SL, Mehrotra B, Rosenberg TJ, et al. Osteonecrosis of the jaws associated with the use of bisphosphonates: a review of 63 cases. J Oral Maxillofac Surg. 2004; 62:527–34. [PubMed: 15122554]

6. Kollet O, Dar A, Shivtiel S, et al. Osteoclasts degrade endosteal components and promote mobilization of hematopoietic progenitor cells. Nat Med. 2006; 12:657–64. [PubMed: 16715089]

7. Miyamoto T, Ohneda O, Arai F, et al. Bifurcation of osteoclasts and dendritic cells from common progenitors. Blood. 2001; 98:2544–54. [PubMed: 11588053]

8. Pierce AM, Lindskog S. Evidence for capping of Fc gamma receptors on osteoclasts. Calcif Tissue Int. 1986; 39:109–16. [PubMed: 2943377]

9. Rothe L, Collin-Osdoby P, Chen Y, et al. Human osteoclasts and osteoclast-like cells synthesize and release high basal and inflammatory stimulated levels of the potent chemokine interleukin-8. Endocrinology. 1998; 139:4353–63. [PubMed: 9751519]

10. Yao Z, Xing L, Qin C, et al. Osteoclast precursor interaction with bone matrix induces osteoclast formation directly by an interleukin-1-mediated autocrine mechanism. J Biol Chem. 2008; 283:9917–24. [PubMed: 18250170]

11. Li H, Hong S, Qian J, et al. Cross talk between the bone and immune systems: osteoclasts function as antigen-presenting cells and activate CD4+ and CD8+ T cells. Blood. 116:210–7. [PubMed: 20304810]

12. Horner A, Bord S, Kelsall AW, et al. Tie2 ligands angiopoietin-1 and angiopoietin-2 are coexpressed with vascular endothelial cell growth factor in growing human bone. Bone. 2001; 28:65–71. [PubMed: 11165944]

13. Haeusler G, Walter I, Helmreich M, et al. Localization of matrix metalloproteinases, (MMPs) their tissue inhibitors, and vascular endothelial growth factor (VEGF) in growth plates of children and adolescents indicates a role for MMPs in human postnatal growth and skeletal maturation. Calcif Tissue Int. 2005; 76:326–35. [PubMed: 15868281]

14. Coxon FP, Thompson K, Roelofs AJ, et al. Visualizing mineral binding and uptake of bisphosphonate by osteoclasts and non-resorbing cells. Bone. 2008; 42:848–60. [PubMed: 18325866]

15. Cackowski FC, Anderson JL, Patrene KD, et al. Osteoclasts are important for bone angiogenesis. Blood. 115:140–9. [PubMed: 19887675]

16. Croucher PI, De Hendrik R, Perry MJ, Hijzen A, et al. Zoledronic acid treatment of 5T2MM-bearing mice inhibits the development of myeloma bone disease: evidence for decreased osteolysis, tumor burden and angiogenesis, and increased survival. J Bone Miner Res. 2003; 18:482–92. [PubMed: 12619933]

17. Yaccoby S, Pearse RN, Johnson CL, et al. Myeloma interacts with the bone marrow microenvironment to induce osteoclastogenesis and is dependent on osteoclast activity. Br J Haematol. 2002; 116:278–90. [PubMed: 11841428]

18. Yamashita J, Datta NS, Chun YH, et al. Role of Bcl2 in osteoclastogenesis and PTH anabolic actions in bone. J Bone Miner Res. 2008; 23:621–32. [PubMed: 18086008]

19. Dobson KR, Reading L, Haberey M, et al. Centrifugal isolation of bone marrow from bone: an improved method for the recovery and quantitation of bone marrow osteoprogenitor cells from rat tibiae and femurae. Calcif Tissue Int. 1999; 65:411–3. [PubMed: 10541770]

20. Enlow DH. Osteocyte necrosis in normal bone. J Dent Res. 1966; 45:213. [PubMed: 4955384]

21. Hale LV, Galvin RJ, Risteli J, et al. PINP: a serum biomarker of bone formation in the rat. Bone. 2007; 40:1103–9. [PubMed: 17258520]

22. Oreffo RO, Mundy GR, Seyedin SM, et al. Activation of the bone-derived latent TGF beta complex by isolated osteoclasts. Biochem Biophys Res Commun. 1989; 158:817–23. [PubMed: 2920041]

23. Utku N, Heinemann T, Tullius SG, et al. Prevention of acute allograft rejection by antibody targeting of TIRC7, a novel T cell membrane protein. Immunity. 1998; 9:509–18. [PubMed: 9806637]
24. Quarello P, Forni M, Barberis L, et al. Severe malignant osteopetrosis caused by a GL gene mutation. J Bone Miner Res. 2004; 19:1194–9. [PubMed: 15177004]
25. Taylor PR, Martinez-Pomares L, Stacey M, et al. Macrophage receptors and immune recognition. Annu Rev Immunol. 2005; 23:901–44. [PubMed: 15771589]
26. Nannuru KC, Futakuchi M, Varney ML, et al. Matrix metalloproteinase (MMP)-13 regulates mammary tumor-induced osteolysis by activating MMP9 and transforming growth factor-beta signaling at the tumor-bone interface. Cancer Res. 70:3494–504. [PubMed: 20406980]
27. Singh S, Singh UP, Grizzle WE, et al. CXCL12-CXCR4 interactions modulate prostate cancer cell migration, metalloproteinase expression and invasion. Lab Invest. 2004; 84:1666–76. [PubMed: 15467730]
28. Lester KS. The unusual nature of root formation in molar teeth of the laboratory rat. J Ultrastruct Res. 1969; 28:481–506. [PubMed: 5822668]
29. Pietrokovski J, Massler M. Ridge remodeling after tooth extraction in rats. J Dent Res. 1967; 46:222–31. [PubMed: 5226389]
30. Rothmann C, Barshack I, Kopolovic J, et al. Spectrally resolved morphometry of the nucleus in hepatocytes stained by four histological methods. Histochem J. 1998; 30:539–47. [PubMed: 9792271]
31. Green JR. Chemical and biological prerequisites for novel bisphosphonate molecules: results of comparative preclinical studies. Semin Oncol. 2001; 28:4–10. [PubMed: 11346859]
32. Kobayashi Y, Hiraga T, Ueda A, et al. Zoledronic acid delays wound healing of the tooth extraction socket, inhibits oral epithelial cell migration, and promotes proliferation and adhesion to hydroxyapatite of oral bacteria, without causing osteonecrosis of the jaw, in mice. J Bone Miner Metab. 28:165–75. [PubMed: 19882100]
33. Peyruchaud O, Winding B, Pecheur I, et al. Early detection of bone metastases in a murine model using fluorescent human breast cancer cells: application to the use of the bisphosphonate zoledronic acid in the treatment of osteolytic lesions. J Bone Miner Res. 2001; 16:2027–34. [PubMed: 11697798]
34. Fournier P, Boissier S, Filleur S, et al. Bisphosphonates inhibit angiogenesis in vitro and testosterone-stimulated vascular regrowth in the ventral prostate in castrated rats. Cancer Res. 2002; 62:6538–44. [PubMed: 12438248]
35. Santini D, Vincenzi B, Dicuonzo G, et al. Zoledronic acid induces significant and long-lasting modifications of circulating angiogenic factors in cancer patients. Clin Cancer Res. 2003; 9:2893–7. [PubMed: 12912933]
36. Tas F, Duranyildiz D, Oguz H, et al. Effect of zoledronic acid on serum angiogenic factors in patients with bone metastases. Med Oncol. 2008; 25:346–9. [PubMed: 18204821]
37. Maruyama K, Asai J, Ii M, et al. Decreased macrophage number and activation lead to reduced lymphatic vessel formation and contribute to impaired diabetic wound healing. Am J Pathol. 2007; 170:1178–91. [PubMed: 17392158]
38. Li D, Gromov K, Proulx ST, et al. Effects of antiresorptive agents on osteomyelitis: novel insights into the pathogenesis of osteonecrosis of the jaw. Ann N Y Acad Sci. 2010; 1192:84–94. [PubMed: 20392222]
39. Singer AJ, Clark RA. Cutaneous wound healing. N Engl J Med. 1999; 341:738–46. [PubMed: 10471461]
40. Cardoso L, Herman BC, Verborgt O, et al. Osteocyte apoptosis controls activation of intracortical resorption in response to bone fatigue. J Bone Miner Res. 2009; 24:597–605. [PubMed: 19049324]
41. Huja SS, Beck FM. Bone remodeling in maxilla, mandible, and femur of young dogs. Anat Rec (Hoboken). 2008; 291:1–5. [PubMed: 18085627]
42. Allen MR, Burr DB. Mandible matrix necrosis in beagle dogs after 3 years of daily oral bisphosphonate treatment. J Oral Maxillofac Surg. 2008; 66:987–94. [PubMed: 18423290]

43. Zwolak P, Manivel JC, Jasinski P, et al. Cytotoxic effect of zoledronic acid-loaded bone cement on giant cell tumor, multiple myeloma, and renal cell carcinoma cell lines. J Bone Joint Surg Am. 92:162–8. [PubMed: 20048108]

44. Sminia T, Dijkstra CD. The origin of osteoclasts: an immunohistochemical study on macrophages and osteoclasts in embryonic rat bone. Calcif Tissue Int. 1986; 39:263–6. [PubMed: 3098388]

45. Weinstein RS, Roberson PK, Manolagas SC. Giant osteoclast formation and long-term oral bisphosphonate therapy. N Engl J Med. 2009; 360:53–62. [PubMed: 19118304]

46. Falanga PB, Blom-Potar MC, Bittoun P, et al. Selection of ovine PrP high-producer subclones from a transfected epithelial cell line. Biochem Biophys Res Commun. 2006; 340:309–17. [PubMed: 16364256]

47. Landesberg R, Cozin M, Cremers S, et al. Inhibition of oral mucosal cell wound healing by bisphosphonates. J Oral Maxillofac Surg. 2008; 66:839–47. [PubMed: 18423269]

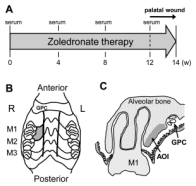

Fig. 1.

Study design, palatal wounds and bone area of interest. **A:** Serum was collected at 0, 4, 8, and 12 weeks after the initiation of zoledronate therapy. The palatal bone was exposed to the oral cavity at 12 weeks after the initiation of zoledronate administration. Zoledronate therapy continued until the end of study (week-14). **B:** The palatal mucosa confined by the rugae, the first molar (M1), and the great palatine canal (GPC) was excised and the alveolar bone denuded (gray-colored area). **C:** The alveolar bone was assessed for osteocyte lacunae at the study end. Area of interest (AOI) was defined as the bone area within 1.0mm from the alveolar bone surface and between the M1 and GPC.

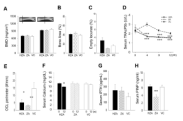

Fig. 2.

Effects of zoledronate therapy for 14 weeks on long bones and serum chemistries. **A:** BMD of the trabecular and cortical bone of the femur was determined at the 20% and 50% position, respectively, of the bone length from the proximal end using pQCT. **B:** Bone area (%) was measured histomorphometrically in the proximal tibiae. **C:** The ratio of the number of empty osteocyte lacunae to the total number of osteocyte lacunae was calculated in the cortex of the proximal tibiae. No significant increase or decrease in zoledronate-treated rats was noted when compared to control. **D:** Mean serum TRAcP5b levels were determined every 4 weeks. The serum TRAcP5b levels were significantly lower in ZA and HZA rats than control. **E:** Osteoclast numbers per linear perimeter in the proximal tibiae were significantly less in HZA and ZA rats than controls. **F:** Mean serum calcium levels were measured at day-0 and week-12. Significant reduction was observed in HZA rats. **G:** Intact PTH levels were measured in the week-12 serum. **H:** Serum P1NP levels were assessed at week-12. Significant decrease was found in ZA rats compare to control. All data represent mean ± SE, n=8/group. One-way ANOVA was used for the statistical analysis except for serum calcium (paired samples t-test). *$p < 0.05$, **$p < 0.01$, ***$p < 0.001$.

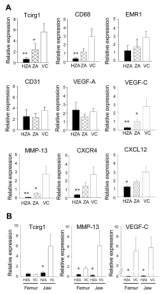

Fig. 3.

Bone marrow cellular responses to zoledronate. **A:** Effects of zoledronate administration for 14 weeks on the marrow of the long bone was determined in senile rats. The bone marrow was harvested from the humeri and RNA isolated. The expression of Tcirg1, CD68, EMR1, CD31, VEGF-A, VEGF-C, MMP-13, CXCR4, and CXCL12 were assessed using qRT-PCR with 18S used for normalization. **B:** Gene expression for Tcirg1, MMP-13, and VEGF-C in the bone marrow was compared between the femur and jaw. Zoledronate was administered for 10 days to young rats and RNA isolated from the bone marrow of the femurs and mandibles. All data represent mean ± SE (n=8/group). *$p < 0.05$, **$p < 0.01$ by one-way ANOVA.

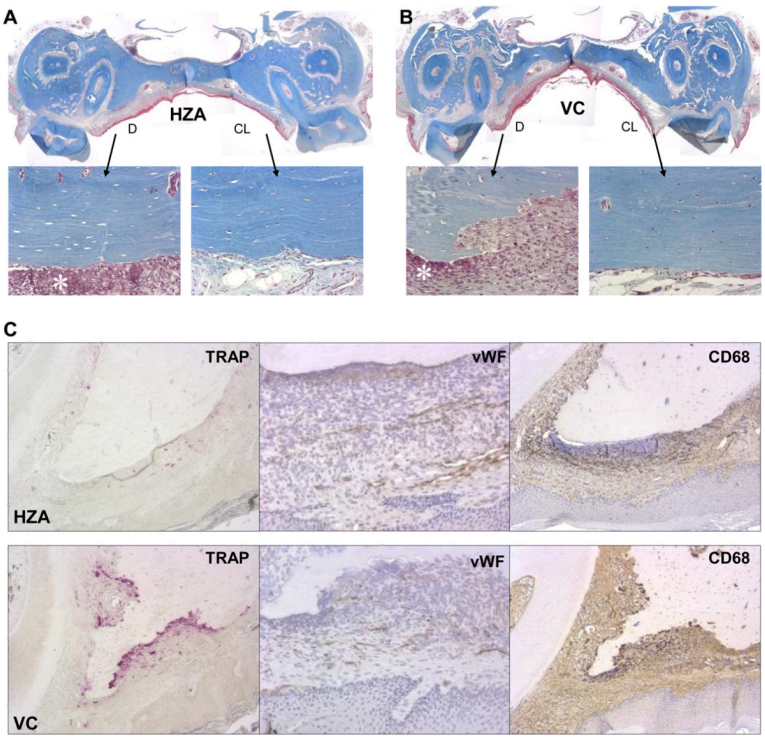

Fig. 4.

Wound healing in the palate. The palatal alveolar bone was denuded 12 weeks after the initiation of zoledronate treatment (see Figure 1). Healing at 2 weeks post-op was evaluated. Representative photomicrographs of Masson's trichrome-stained sections of the palates of rats treated with high-dose zoledronate **(A)** and vehicle control **(B)** (40x). Epithelialization of wounds was observed in most cases. The denuded (D) and contralateral intact (CL) sides are magnified (200x) to show osteocyte lacunae. Neutrophil aggregation (*) was noted next to the unresorbed bone surfaces. **C:** Histological staining for osteoclasts (TRAP) (100x), von Willebrand factor positive endothelial cells (vWF) (200x), and macrophages/monocytes (CD68) (100x). TRAP+ cells are shown in red color and vWF+ cells and CD68+ cells in brown color. The denuded alveolar bone areas in the HZA (top row) and in the VC (bottom row) are shown.

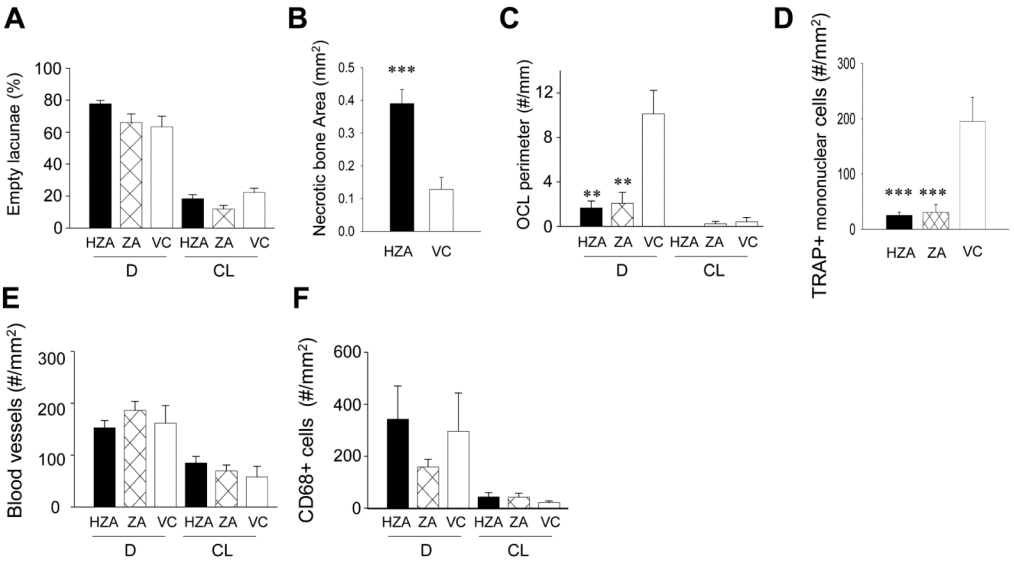

Fig. 5.

Histomorphometric assessement of wound healing. **A:** The percentage of empty osteocyte lacunae in the predefined AOI in the palate was determined histomorphometrically. **B:** The entire necrotic bone area was histomorphometrically measured and compared between HZA and VC. **C:** Osteoclast numbers per linear perimeter were measured in the AOI. In the denuded site significant decrease was noted in HZA and ZA compared to control rats. **D:** The number of TRAP+ mononuclear cells per mm^2 was determined in the connective tissue area in the denuded site. Significant reduction in preosteoclast numbers was found in HZA and ZA compared to control rats. The numbers of vWF positive blood vessels **(E)** and CD68 positive cells **(F)** were assessed in the connective tissue. Data are shown as mean ± SE (n=8/group). $^{**}p < 0.01$, $^{***}p < 0.001$ by one-way ANOVA.